HHS Public Access

Author manuscript

ASAIO J. Author manuscript; available in PMC 2015 July 01.

Published in final edited form as:

ASAIO J. 2014 ; 60(4): 391–399. doi:10.1097/MAT.0000000000000093.

Control of respiration-driven retrograde flow in the subdiaphragmatic venous return of the Fontan circulation

M Vukicevic[1], **T Conover**[1], **M Jaeggli**[1], **J Zhou**[1], **G Pennati**[2], **TY Hsia**[3], and **RS Figliola**[1]

[1]Mechanical and Bioengineering Engineering, Clemson University, Clemson, SC, USA

[2]Bioengineering, Politecnico di Milano, Milan, Italy

[3]Cardiothoracic Surgery, Great Ormond Street Hospital for Children, London, United Kingdom

Abstract

Respiration influences the subdiaphragmatic venous return in the total cavopulmonary connection (TCPC) of the Fontan circulation whereby both the inferior vena cava (IVC) and hepatic vein flows can experience retrograde motion. Controlling retrograde flows could improve patient outcomes. Using a patient-specific model within a Fontan mock circulatory system with respiration, we inserted a valve into the IVC to examine its effects on local hemodynamics while varying retrograde volumes by changing vascular impedances. A bovine valved conduit reduced IVC retrograde flow to within 3% of antegrade flow in all cases. The valve closed only under conditions supporting retrograde flow and its effects on local hemodynamics increased with larger retrograde volume. Liver and TCPC pressures improved only while the valve leaflets were closed while cycle-averaged pressures improved only slightly (italic>1 mm Hg). Increased pulmonary vascular resistance raised mean circulation pressures but the valve functioned and cardiac output improved and stabilized. Power loss across the TCPC improved by 12–15% (pbold>0.05) with a valve. The effectiveness of valve therapy is dependent on patient vascular impedance.

Keywords

respiration; lumped parameter model; Fontan circulation

INTRODUCTION

Respiration can impose a profound influence on the subdiaphragmatic venous return in the total cavopulmonary connection (TCPC) of the single ventricle Fontan circulation.[1–7] The TCPC directly connects the superior and inferior vena cavae (SVC and IVC) to the pulmonary arteries, resulting in the total venous return flowing passively into the pulmonary circulation. Lacking the ventricular power source, the systemic venous pressure and the respiratory mechanics become the dominant forces for moving pulmonary blood flow.

Corresponding author: R. Figliola, 247 Fluor Daniel Building, Clemson, SC 29634, fgliola@clemson.edu, (864) 656 – 5635, (864) 656 – 7299 (FAX).

Conflicts of Interest: None declared

Disclosures: Financial support of Fondation Leducq and NIH (Grant HL083975)

Respiration-gated magnetic resonance (MR) imaging[1–3,5–7] has revealed significant differences to the ECG-triggered acquisitions often applied in modeling studies.[5] Venous and pulmonary arterial flows increase during inspiration and decrease in expiration.[1–3] This pattern is particularly accentuated in the inferior venous return[1–7] due to the recoil of the thoracic cage during expiration and the absence of a venous valve.[2] For many patients, as inspiration wanes, both the inferior vena cava (IVC) and hepatic vein (HV) flows can experience a period of retrograde motion away from the heart.

Late complications of the failing Fontan circulation include problems in the liver and gastrointestinal tract.[2,3] The idea of implanting a valve in the IVC originated with Fontan and Baudet.[8] Hsia et al.[2] suggested a valve to reduce hepatic congestion. Baslaim[9] and Zureikad et al.[10] reported reduced retrograde HV flows following xenograft conduit implantation. Prenger et al.[11] reported positive outcomes with porcine-valved Dacron conduits and Corno et al.[12] demonstrated using self-expandable valved stents in the IVC. There are only limited clinical or realistic experimental results on which to discern between the hemodynamic advantages and penalties imposed on the circulation when using a valve.

A consequence of the Fontan circulation is elevated venous pressure associated with subnormal cardiac output. Systemic venous hypertension is known to lead to cirrhosis, liver failure, and portal hypertension.[13] Pulmonary vascular resistance (PVR) is cited as the single most important factor limiting cardiac output (CO) in the Fontan circulation and changes with growth and age, [13,14] but its role in subdiaphragmatic venous return is largely undocumented.[15] The retrograde to antegrade flow volumes can vary markedly between patients,[1–3,5,16] which implicates pulmonary vascular compliance (PVC) and circulation impedance.[17]

Multi-domain models couple a lumped parameter (LP) network of the circulation with a higher dimensional model of the anastomosis site. Several numerical models have been developed to predict patient differences in single ventricle physiologies,[18,19] including models with respiration.[20] Others have used LP flow loops to assess innovative cardiopulmonary assist devices.[16,21–23] The effects of TCPC flow resistance on cardiac output were reported using an LP-coupled numerical model.[24]

Vukicevic et al. [25] described a multi-domain mock circulatory system (MCS) of the Fontan circulation, which included respiration and aortic pulsatility. We use this in vitro model to study the impact of valve therapy on subdiaphragmatic venous hemodynamics.[25] Systems-level impedances and respiration pressures are included to properly model the time-dependent response within the thorax and abdomen. We evaluate the impact of a valve on reducing retrograde volume, improving antegrade flow, and reducing venous pressures and flow power losses.

MATERIALS AND METHODS

The mock circulatory system (MCS) of the Fontan circulation system is a physical realization of four branches of circulation coupling an LP network with an anatomically accurate, three-dimensional TCPC test section, as shown in the schematic of Figure 1a and

the photograph of Figure 1b.[25] The system is tuned to a particular physiological state using generic reference values for each impedance element scaled by body surface area (BSA) and then adjusted with available patient-specific clinical information.[18,19] A ventricular-assist device (VAD) (Excor®, 80 cc, Berlin, Germany) develops the pulsatile aortic pressure. Atrial pressure is maintained constant. Time-dependent thoracic (intrapleural) and abdominal respiration pressures (P_{th} and P_{ab}) associated with normal breathing are applied simultaneously to compliant elements within the thoracic cavity (pulmonary, TCPC, IVC) and the abdomen.

The TCPC test section is a patient-specific geometry based on MR images and realized using a thin walled (1±0.2 mm), compliant (C ~ 0.28mL/mmHg) silicone phantom (Shelley Medical, Canada). Residual arterial and venous compliances were distributed between the surrounding compliance elements.[25] The tested valve was an 18 mm pulmonary valved conduit (CVC) (Contegra 200, Medtronic, Inc., Minneapolis, MN). When inserted, it formed part of the IVC downstream of the IVC/HV junction. Valve function was verified by borescope.

Flow rates were measured with electromagnetic probes (Carolina Medical Electronics, King, NC). Pressures were measured using liquid-filled catheters and transducers (DTXplus, BD Medical Systems, Sandy, UT). System operation was controlled using a data acquisition/control board (USB 6211/Labview; National Instruments, Austin, TX). A saline-glycerin blood analog was used (1060 kg/m^3, 3.3 x 10^{-6} m^2/s at 22°C).

Flow volumes were calculated by integrating the flow towards (antegrade) or away from (retrograde) the heart during a full respiration cycle. Power loss across the TCPC test section was calculated by integrating instantaneous total pressure, *P*, and flow rate, *Q*, over the respiration cycle

$$\dot{W} = (P_t Q)_{IVC} + (P_t Q)_{SVC} - (P_t Q)_{RPA} - (P_t Q)_{LPA}$$

where $P_t = P + \frac{1}{2}\rho(\frac{Q}{A})^2$ with *Q* based on the cycle average.

Setup

Clinical studies report that flow pulsatility and retrograde flow volumes vary markedly between patients.[1–3,6,16] Both were varied here either by changing the pulmonary compliance or by changing pulmonary resistance. We established one patient-specific baseline condition in the MCS (EXP). Four additional conditions were created by increasing effectively the patient's PVC by 25% (PVC25) and 50% (PVC50) with PVR fixed, and by increasing PVR (done by increasing R_{rld} and R_{lld}) by 33% (PVR33) and 90% (PVR90) with PVC fixed. The values used for the five test conditions are representative of patients having a functional Fontan.[15,21,24]

The patient modeled was a 10.8 year-old female, 7-years post-lateral tunnel with no fenestration, BSA = 1.3 m^2. Clinical CO was 3.3 L/min at a HR = 80 bpm, PVR of 2.1 WU,

SVR of 18.2 WU, and respiration rate RR of 17.1 breaths/min (t_R = 3.51 s). The clinical MR velocity maps acquired were gated on respiration over a full respiration cycle.[7]

The patient-specific baseline conditions (EXP) were set by adjusting the LP elements values (Table 1) to match clinical data. The applied thoracic and abdominal respiration pressure waveforms (Fig. 2a) were adopted from West[26] under quiet breathing[26–28] over the respiration period t_R. The model consists of an active inspiration period ($0 < t/t_R < t_{insp}/t_R$), followed by a passive expiration period. The thoracic and abdominal pressures, P_{th} and P_{ab}, were bounded between −1 to −5 mm Hg and 0 to 4 mm Hg, respectively.[28,29] The ascending aortic pressure applied is shown in Fig. 2b. The mean aortic pressure was fixed at 75 mm Hg and the atrial pressure was fixed at 7 mm Hg. Baseline PVC was tuned to 4.32 mL/mm Hg with t_{insp}/t_R = 0.4 to meet clinical flow pulsatility.

The clinical (MR) IVC and SVC flow rates are shown with the experimental flow rates used (EXP) in Fig. 2c and Fig. 2d. The resulting antegrade and retrograde IVC flow volumes agree to within 8% and 1% and the SVC mean flow rate to within 1% of the clinical measurements. The four additional test conditions were developed from this baseline.

Uncertainty Statement

Statistical values reported are ensemble averages over 20 contiguous respiration cycles. The uncertainty in a reported mean flow rate is ±0.7%, in differential pressure is ±0.3 mm Hg, and in retrograde flow volume is ±0.5 mL, each at a 95% confidence and evaluated as reported previously.[25]

Results

PVC Effects

Flow rate and pressure signals are compared in Figure 3 for each case (EXP, PVC25, PVC50) both without (baseline) and with the valve. Corresponding results are given in Table 2. These three baseline cases provided progressively increasing flow pulsatility, noted by Q_{retro}/Q_{ante}, with increasing IVC and HV antegrade and retrograde flow volumes while CO was kept constant.

Implanting the valve decreased IVC retrograde flow volumes by 54%, 72%, and 67% (Fig. 3a–c, Table 2) compared to the respective no valve baselines. IVC antegrade flow volumes also decreased while overall IVC mean flow rates remained unchanged ($p<0.05$). Retrograde flow volumes within the HV decreased by 5%, 33%, and 32%, respectively (Fig. 3d–f, Table 2) over baselines while mean flow rates remained unchanged.

Flow and pressure waveforms were time-dependent. IVC and HV antegrade flows (Fig. 3a–f) were largely unchanged over the inspiration period ($0< t/t_R < 0.4$) between corresponding baseline and valve cases. Following an initial closing leakage, the valve closed blocking retrograde flow ($0.47 < t/t_R < 0.6$). The valve reopened with the resumption of antegrade flow ($0.65 < t/t_R < 1$) but the increases in flow rate over this period were reduced with the valve present. Over a full cycle, IVC flow pulsatility was controlled to within 3% in each case.

TCPC and liver pressures (Fig. 3g–3l) dropped gradually over the inspiration period ($0< t/t_R < 0.4$) in each case. With the onset of expiration ($t/t_R \sim 0.4$), the IVC pressure rose abruptly whereas the liver pressure rose more gradually. Without a valve, this developed the pressure gradient necessary for retrograde flow (Fig. 3a–3f). The valve was closed by the retrograde volume ($0.47 < t/t_R < 0.6$), during which TCPC junction pressures increased and liver pressures decreased. Closure was accompanied by short duration ($0.47 < t/t_R < 0.7$) pressure oscillations during which TCPC pressures rose by up to 6 mm Hg and liver pressures decreased by 5.5 mm Hg below corresponding baseline values. The valve stayed closed for the 12 to 15% of the respiration cycle consistent with conditions supporting retrograde flow.

Pressure changes across the valve are shown in Fig. 4(a)–(c). With expiration, pressures on the downstream side of the valve (IVC) abruptly increased consistent with valve closing. Concurrently, pressures at the HV confluence upstream of the valve showed decreased pressure. A 2 mm Hg (root-mean-square) gradient prevailed across the closed valve. With the valve implanted, power losses (Table 2) across the TCPC were reduced by 10 to 12% ($p < 0.05$).

PVR Effects

PVR was increased from the baseline of 2.1 WU (EXP) to 2.8 WU and 4.0 WU (PVR33, PVR90). With constant compliance, the amount of blood volume moved by respiration did not change between cases. Flow and pressure waveforms are compared both with and without the valve in Fig. 5a–l with statistical values shown in Table 3. Without a valve, increasing PVR augmented flow pulsatility, raised all system pressures, and cardiac output dropped. Retrograde flow volumes increased by 49% and 120% and mean system pressures increased by 10% and 29%, respective to baseline. Duration of retrograde flow lengthened from 10% (EXP) to 16% (PVR90) of a respiration cycle.

The implanted valve decreased and stabilized IVC retrograde flow volumes to within 3% of antegrade flow (Fig. 5b–c, Table 3). With elevated PVR, overall IVC antegrade flow remained nearly constant (PVR33, PVR90) so that the net mean IVC flow increased. For these cases, antegrade flow during late expiration remained about the same with or without the valve. Retrograde flow volumes within the HV decreased to within 20–26% of antegrade flow (Fig. 5d–f, Table 3) while mean flow rates remained unchanged. CO remained constant between cases with a valve ($p<0.05$).

Cycle-averaged mean TCPC and liver pressures were essentially unchanged between valve and no valve cases ($p < 0.05$). TCPC and liver pressures (Fig. 5g–5l) dropped gradually over the inspiration period ($0< t/t_R < 0.4$) in all cases. With the onset of expiration ($t/t_R \sim 0.4$), the IVC pressure rose abruptly whereas the liver pressure rose more gradually.

DISCUSSION

This study provides a systems-level approach to understanding the potential outcomes of introducing IVC valve therapy into the Fontan circulation. The novel design of our system treats respiration and allows for interaction between abdomen and thorax. The system model recapitulates the respiratory-dependent flow reversal in the inferior venous return in the

TCPC observed clinically.[1–7] By changing impedance values, we achieved different levels of pulsatility and retrograde blood volume with which to compare the hemodynamic benefits of using a valve. As many of the late Fontan attrition relate to hepatic dysfunction and gastrointestinal protein losing entropathy (PLE), the model not only allows for mechanistic insight into the abnormal flow circulation in Fontan patients, but also provides a platform to examine the benefit of controlling or limiting the flow reversal into both the systemic inferior venous and the splanchnic circulation. The study demonstrates that there is a flow benefit with minimal pressure penalty to limiting the respiration-dependent flow reversal using clinically available valve prostheses. As future valve materials develop, our findings identify mechanisms involved and needed towards advancing valve therapy. The study establishes a clinical rationale to further examine surgical or interventional methods that can limit the observed flow reversal in Fontan patients, in particular those who suffer from liver cirrhosis or protein losing entropathy. For example, in patients with high PVR, and thus not transplantation candidates, and failing Fontan due to PLE, the implantation of a valve in the inferior pathway may lead to a more efficient splanchnic venous return and resolution of PLE. We did not test the valve materials for thrombogenic potential and our findings are not intended as clinical recommendations. Interactions between thoracic and abdominal respiration pressures with the various associated compliance elements were shown to influence the IVC flow direction and result in retrograde flows. The implanted valve reduced IVC retrograde flow significantly while decreasing liver pressures during the 10 to 16% of the respiration cycle that the valve remained closed. With the valve closed, TCPC pressures increased and liver pressures decreased. Valve closure was assisted by the inertia of retrograde flow volume. Valve closure time corresponded with the period supporting retrograde motion within the IVC so exact times would change with breathing rhythm. The valve reduced power losses across the TCPC by a modest 10–12% over a respiration cycle. These results are favorable and the improvements more apparent in cases with higher retrograde volume.

Compliance changes served to increase pulsatility by increasing the blood volume moved by respiration pressures between successive cases. The reduction in retrograde flow associated with using a valve was found to be offset by physiological responses that also decreased antegrade flow during late expiration. This limited net gains in antegrade flow from using a valve. By incorporating the splanchnic circulation in our model, we found that the combinations of reduced retrograde flow towards the liver coupled with higher pressures in the TCPC and lower pressures in the hepatic vein, each served to reduce the driving force for antegrade flow during late expiration. This demonstrated reduced liver loading during expiration as a consequence of valve therapy. In changing PVR, the compliance and respiration pressures were fixed so that the amount of blood volume moved by respiration did not change between cases. Accordingly, late expiration behavior remained essentially the same between cases. The overall IVC antegrade flow stabilized with a valve and retrograde flow reduced. Progressive increases in PVR demonstrated elevated venous pressures. Liver disease is an unfortunate consequence of the Fontan circulation due to elevated venous pressures and reduced cardiac output. Unfortunately, the valve did little to reduce mean liver pressures offering only short duration decreases during valve closure. Notably, valve therapy served to stabilize cardiac output with increasing PVR.

Corno et al.[12] also found that a valve implanted in the IVC of healthy adult pigs functioned better with higher retrograde flow volumes. Santhananakrishnan et al.[31] used a flow loop with aortic pulsatility applied directly to the vena cava to study valve function. In their study, respiration and circulation impedances were neglected with the only compliance being a passive TCPC model. They reported that the valve functioned on the cardiac cycle with remarkable improvements in overall hemodynamics. Clinical studies report differing outcomes following implantation of a valved conduit. Baslaim[9] reported that 15 of 18 patients at 48 months showed reduction in retrograde flows, with good oxygen saturation, without thromboembolic episodes, and with good ventricular function. Zureikad et al.[10] reported positive results for five patients. However, Schoof et al.[32] reported localized thrombosis in three patients.

For a functional Fontan circulation, the retrograde flow pulsatility represented by our experimental models (Table 2 and 3) fits within the range of published clinical data. For example, Hsia et al.[2,3] reported measured values of Q_{retro}/Q_{ante} of 6±11% and 27±17% for IVC and HV, respectively, in their respiration study of functional Fontan TCPC patients (N = 31, 14±5 years). Hjordtal et al.[1] reported measured values (N = 11, 12.4± 4.6 years) within the IVC of 10.5±12.4%. Extending the study to the failing Fontan circulation must apply different physiological conditions than modeled here.

Not presented due to space limitations, we found no substantial differences to these results when using different heart rates or modest changes in caval flow splits. While we have noted improved response to valve therapy under forced heavy breathing, a proper model of the physiological changes associated with increased metabolic activity requires substantially changing the lumped parameter values and awaits separate study.

CONCLUSIONS

The hemodynamic behavior of the Fontan circulation in single ventricle physiology is dependent on respiration. Subdiaphragmatic flows often reverse during expiration. We used a patient-specific Fontan mock circulatory system with quite respiration to study the effects of implanting a bovine valved conduit into the inferior vena cava (IVC). We varied system compliance and resistance to vary retrograde volume to study comparative hemodynamics over a respiration cycle.

Overall, the valve reduced the IVC retrograde flow volume to within 3% of antegrade flow volume in all cases. Hepatic vein retrograde flow volumes decreased. Improvements in antegrade flows were moderated by circulation impedances. The valve provided some relief of retrograde loading on the liver during expiration. Pressures within the total cavopulmonary connection (TCPC) increased and liver pressures decreased only during the duration of valve closure. Otherwise, mean IVC and liver pressures improved by less than 1 mm Hg over a respiration cycle. Power losses through the TCPC improved with the valve by 12 – 15%. For the host patient, increasing pulmonary vascular resistance increased mean system pressures regardless of whether a valve was implanted but cardiac output stabilized with a valve. The results show that hemodynamic benefits of valve therapy will depend on patient vascular impedance and physiology.

References

1. Hjortdal VE, Emmertsen K, Stenbog E, et al. Effects of Exercise and Respiration on Blood Flow in Total Cavopulmonary Connection : A Real-Time Magnetic Resonance Flow Study. Circulation. 2003; 108:1227–1231. [PubMed: 12939218]
2. Hsia TY, Khambadkone S, Redington A, et al. Effects of Respiration and Gravity on Infradiaphragmatic Venous Flow in Normal and Fontan Patients. Circulation. 2000; 102:III-148–III-153. [PubMed: 11082378]
3. Hsia TY, Khambadkone S, Bradley S, de Leval M. Subdiaphragmatic venous hemodynamics in patients with biventricular and Fontan circulation after diaphragm plication. J Thorac Cardiovasc Surg. 2007; 134:1397–405. [PubMed: 18023650]
4. Fogel M, Weinberg P, Hoydu A, et al. The nature of flow in the systemic venous pathway in Fontan patients utilizing magnetic resonance blood tagging. J Thorac Cardiovasc Surg. 1997; 114:1032–1041. [PubMed: 9434698]
5. Hart C, Gabbert I, Voges M, et al. New insights in the Fontan circulation: 4-dimensional respiratory and ECG-triggered phase contrast magnetic resonance imaging. J Cardiovascular Magnetic Resonance. 2013; 15(Suppl 1):O38.
6. Penny D, Redington A. Doppler echocardiographic evaluation of pulmonary blood flow after the Fontan operation: the role of the lungs. Br Heart J. 1991; 66:372–374. [PubMed: 1747298]
7. Sondergaard L, Hoschtitzky A, Hsia TY, et al. Respiration synchronized flow quantification in total cavopulmonary connections. Circulation. 2000; 102(18):II–771.
8. Fontan J, Baudet E. Surgical repair of tricuspid atresia. Thorax. 1971; 26:240. [PubMed: 5089489]
9. Baslaim G. Bovine Valved Xenograft (Contegra) Conduit in the Extracardiac Fontan Procedure: The preliminary Experience. J Card Surg. 2008; 23:146–149. [PubMed: 18304129]
10. Zureikat Y, Hyasat BH, Alhusban S, et al. The use of bovine jugular vein in the Fontan circulation. JRMS. 2005; 12:53–56.
11. Prenger KB, Hess J, Cromme-Dijkhuis A, Eijgelaar A. Porcine-valved Dacron conduits in Fontan procedures. Ann Thorac Surg. 1988; 46:526–530. [PubMed: 2973288]
12. Corno AF, Zhou J, Tozzi P, von Segesser L. Off-bypass implantation of a self-expandable valved stent between inferior vena cava and right atrium. Interactive Cardiovascular and Thoracic Surgery. 2003; 2:166–169. [PubMed: 17670018]
13. Fredenburg TB, Johnson TR, Cohen MD. The Fontan Procedure: Anatomy, Complications, and Manifestations of Failure. Radio Graphics. 2011; 31:453–463.
14. Ciliberti P, Schulze-Neick I, Giardini A. Modulation of pulmonary vascular resistance as a target for therapeutic interventions in Fontan patients. Future Cardiology. 2012; 8(2):271–284. [PubMed: 22413985]
15. Mitchell MB, Campbell D, Ivy D, et al. Evidence of pulmonary vascular disease after heart transplantation for fontan circulation failure. J Thorac Cardiovasc Surg. 2004; 128:693–702. [PubMed: 15514596]
16. Dur O, Lara M, Arnold D, et al. Pulsatile In Vitro Simulation of the Pediatric Univentricular Circulation for Evaluation of Cardiopulmonary Assist Scenarios. Artif Organs. 2009; 33:967–76. [PubMed: 20021470]
17. Lankhaar JW, Westerhof N, Faes TJC, et al. Pulmonary vascular resistance and compliance stay inversely related during treatment of pulmonary hypertension. European Heart Journal. 2008; 29:1688–1695. [PubMed: 18349027]
18. Baretta A, Corsini C, Yang W, et al. Virtual surgeries in patients with congenital heart disease: a multiscale modelling test case, *Philosophical transactions*. Series A. 2011; 369:4316–4330.
19. Baretta A, Corsini C, Marsden A, et al. Respiratory effects in patient-specific CFD models of the Fontan circulation. European J Mech B/Fluids. 2012; 35:61–69.
20. Magosso E, Cavalcanti S, Ursino M. Theoretical analysis of rest and exercise hemodynamics in patients with total cavopulmonary connection. Am J Physiol Heart Circ Physiol. 2002; 282:H1018–H1034. [PubMed: 11834500]

21. Dur O, Lara M, Arnold D, et al. Pulsatile In Vitro Simulation of the Pediatric Univentricular Circulation for Evaluation of Cardiopulmonary Assist Scenarios. Artif Organs H. 2009; 33:967–76.
22. Pekkan K, Frakes D, de Zelicourt D, et al. Pediatric Ventricle Assist Devices to the Fontan Circulation: Simulations with a Lumped-Parameter Model. ASAIO Journal. 2005; 51:618–628. [PubMed: 16322728]
23. Rodefeld M, Coats B, Fisher T, et al. Cavopulmonary Assist for the Univentricular Fontan Circulation: von Karman Viscous Impeller Pump. J Thorac Cardiovasc Surg. 2010; 14:529– 536. [PubMed: 20561640]
24. Sundareswaran SK, Pekkan K, Das LP, et al. The total cavopulmonary connection resistance: a significant impact on single ventricle hemodynamics at rest and exercise. Am J Physiol Heart Circ Physiol. 2008; 295:H2427–H2435. [PubMed: 18931028]
25. Vukicevic M, Chiulli J, Figliola RS, et al. Mock Circulatory System of the Fontan Circulation to Study Respiration Effects on Venous Flow Behavior. ASAIO J. 2013; 59(3):253–60. [PubMed: 23644612]
26. West, JB. U Respiratory Physiology. Essentials. 8. Lippencott, U., editor. Williams, and Wilkins; Balimore, MD: 2008.
27. Cavalcanti S, Gnudi G, Masetti P, Ussia GP, Marcelletti CF. Analysis by mathematical model of haemodynamic data in the failing Fontan circulation. Physiol Meas. 2001; 22:209–222. [PubMed: 11236882]
28. Grimby G, Goldman G, Mead J. Respiratory muscle action inferred from rib cage and abdominal V-P partitioning. J Appl Physiol. 1976; 41:739–751. [PubMed: 993162]
29. Sicar, S. U Principles of medical physiology U. Vol. 49. Thieme; Stuttgart, Germany: 2008.
30. Yu JJ, Yun TJ, Yun SC, et al. Low pulmonary vascular compliance predisposes post-Fontan patients to protein-losing enteropathy. Inter J Cardio. 2013; 165:454–457.
31. Santhananakrishnan A, Maher KO, Tang E, et al. Hemodynamic effects of implanting a unidirectional valve in the inferior vena cava of the Fontan circulation pathway. Am J Physiol Heart Circ Physiol. 2013; 305
32. Schoof PH, Koch AD, Hazekamp MG, et al. Bovine jugular vein thrombosis in the Fontan circulation. Thorac Cardiovasc Surg. 2002; 124:1038–40.

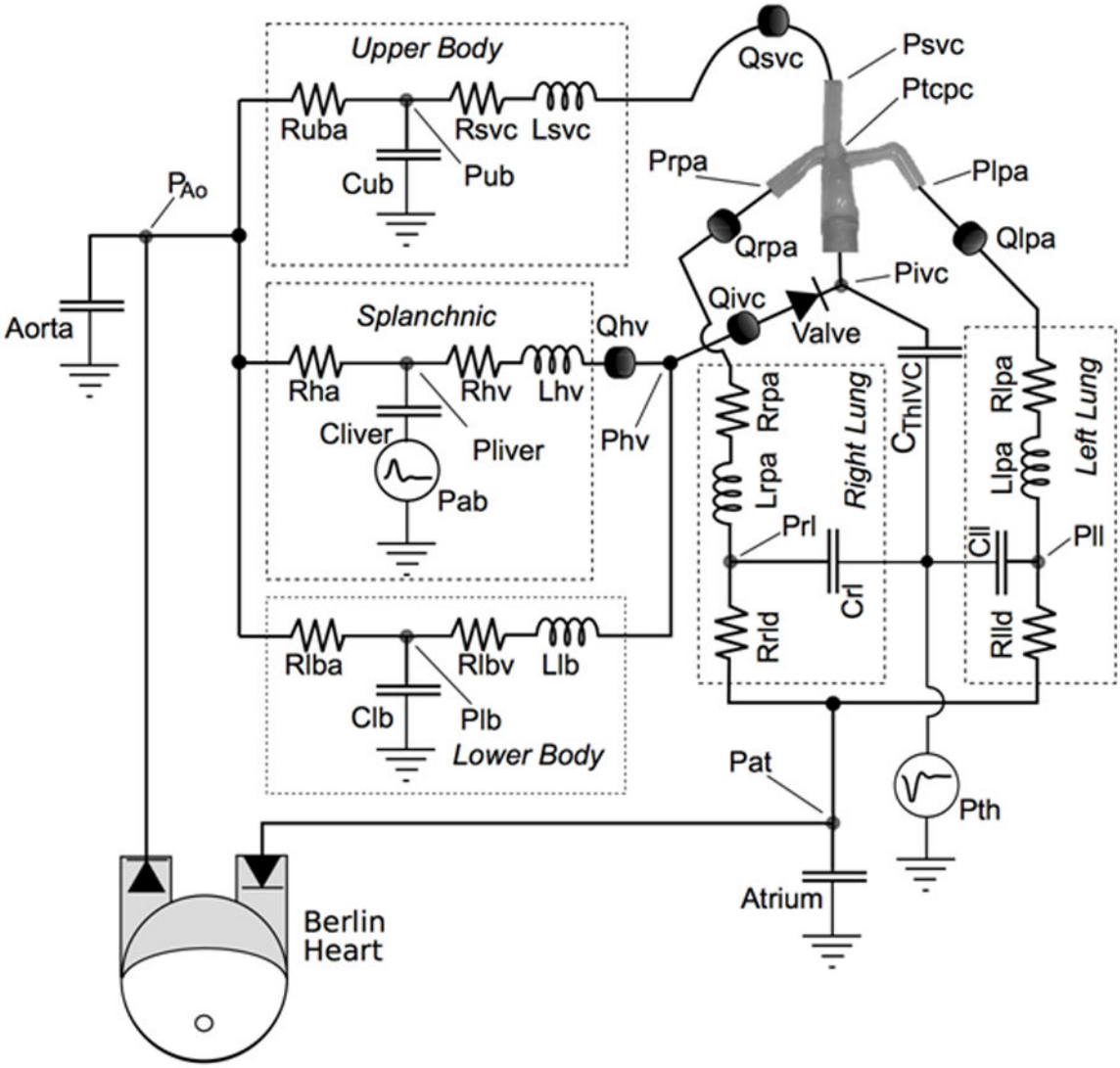

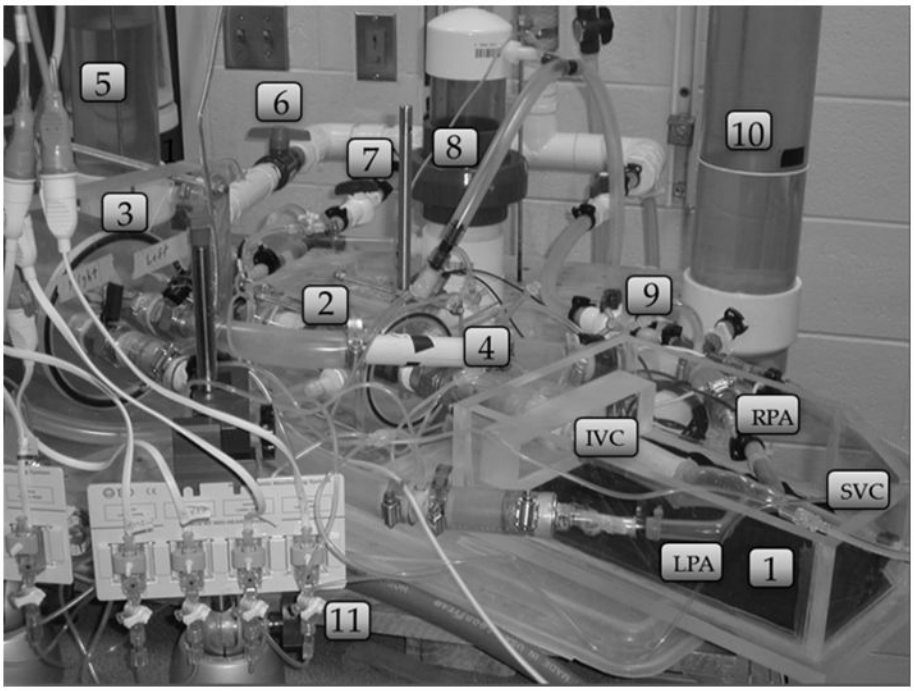

Figure 1.

(a) Lumped parameter model used for the mock circulatory system. (b) Photograph of system: 1-TCPC test section, 2 - IVC compliant element, 3 – pulmonary compliance elements, 4 –pulmonary resistance element, 5, 10 – lower and upper body compliance elements, 6, 7, 9 – resistance elements, 8 – splanchnic compliant element, 11 - pressure transducers.

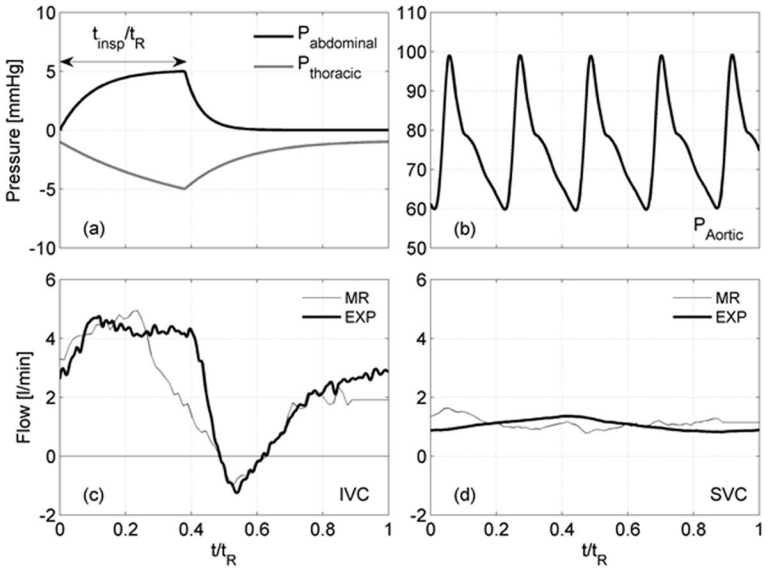

Figure 2.

Waveforms used in the experiments: (a) respiration pressures and (b) aortic pressure. Comparisons of clinical flow waveforms with experimental model: (c) IVC and (d) SVC.

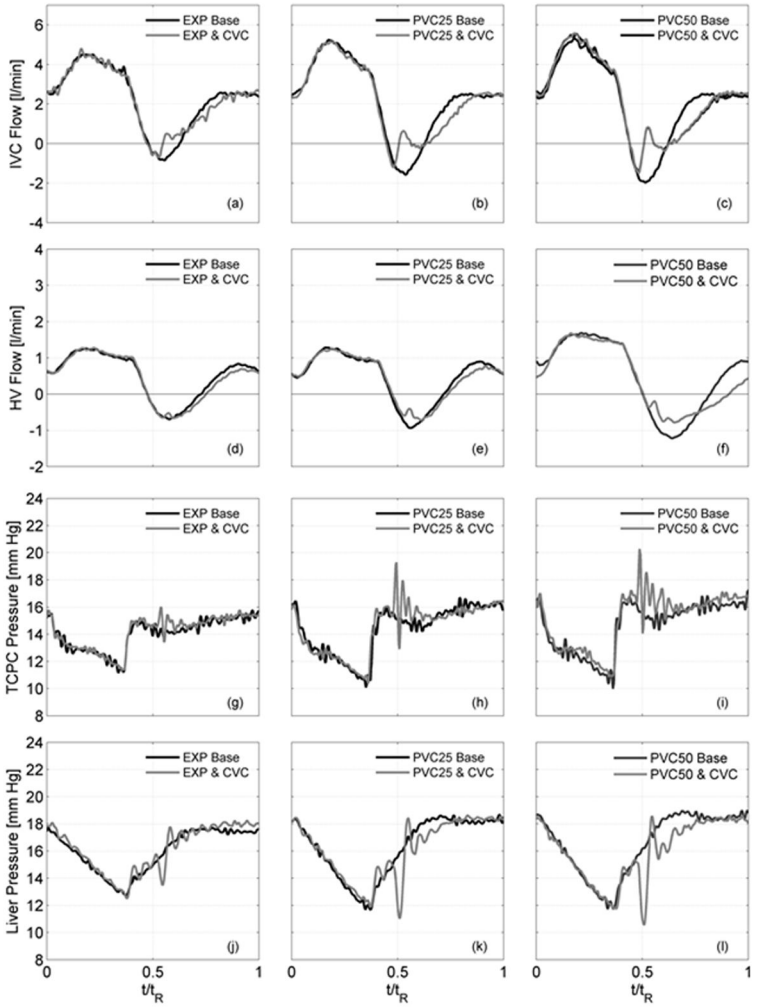

Figure 3.

Hemodynamic flow and pressure signals both without (black lines) and with (gray lines) a bovine valved conduit (CVC) with changing conditions (EXP, PVC25, PVC50): (a–c) IVC flows, (d–f) HV flows, (g–i) TCPC pressure, (j–l) liver pressure.

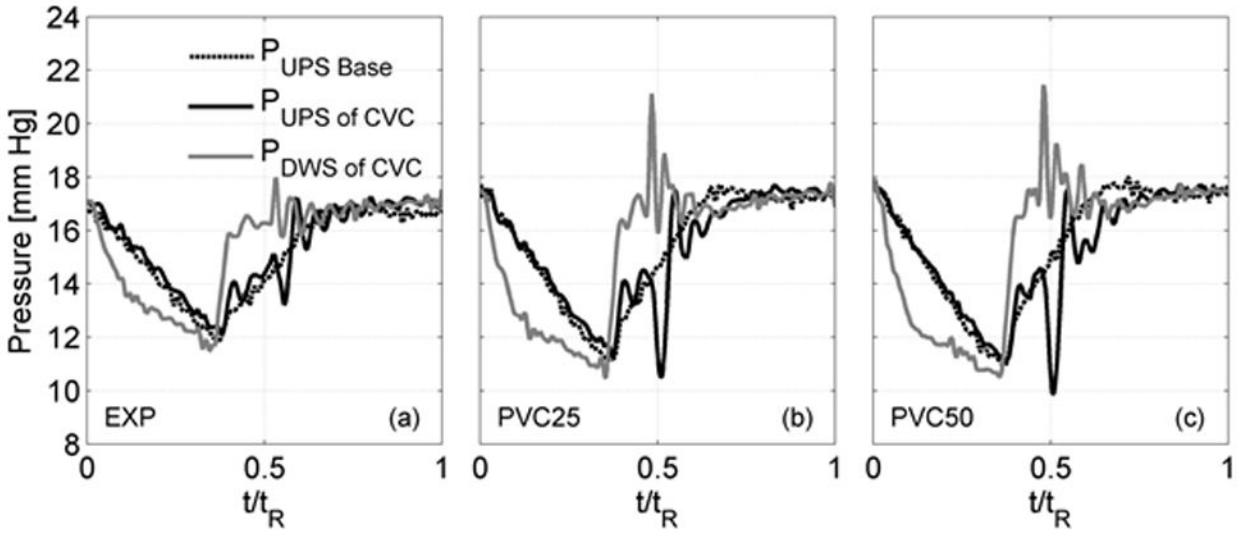

Figure 4.

Measured pressures upstream (hepatic vein confluence) and downstream (inferior vena cava) of a bovine valved conduit (CVC) over one respiration cycle for three testing conditions (EXP, PVC25 and PVC50). Pressure without valve (Baseline) also shown for each case.

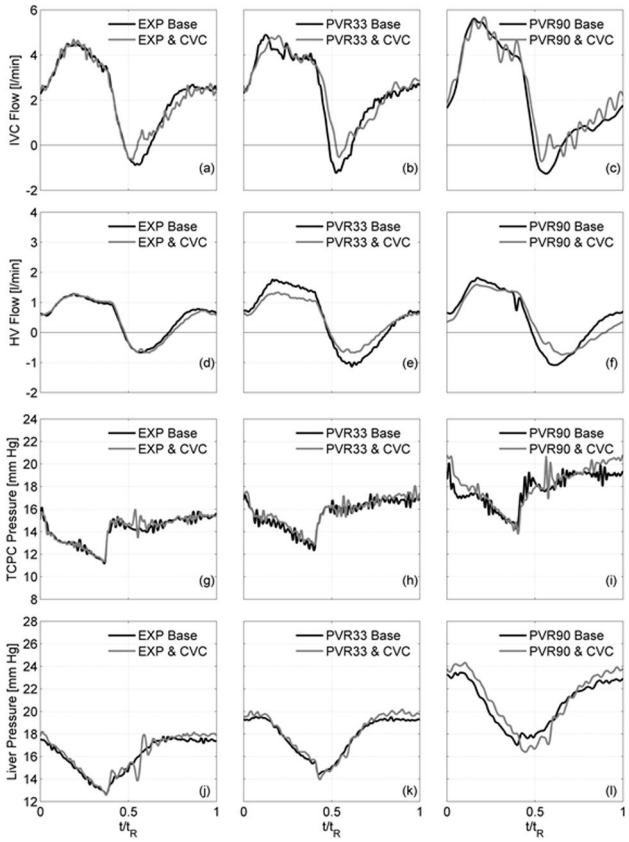

Figure 5.

Hemodynamic flow and pressure signals both between without (black lines) and with (gray lines) a bovine valved conduit (CVC) with increasing PVR: (a–c) IVC flows, (d–f) HV flows, (g–i) TCPC pressure, (j–l) liver pressure

Table 1

Values of the lumped parameter experimental model parameters. Resistances (mm Hg-s/ml); Compliances (ml/mm Hg).

LPN parameters	Patient Specific * BSA=1.3 m^2
Rub	3.27±0.17
Cub	3.12±0.05
Rsvc	0.080±0.002
Rha	7.28±0.23
Cliver	4.41±0.14
Rhv	0.16±0.005
Rlba	2.03±0.12
Clb	3.86±0.12
Rlbv	0.038±0.002
Rrpa	0.034±0.002
Rrld	0.19±0.02
Crl+Crpa	2.15±0.07
Rlpa	0.034±0.002
Rlld	0.19±0.02
Cll+Clpa	2.17±0.07
Civc	2.57±0.08
Ctcpc	0.28±0.05

* 95% level of confidence

Table 2

Hemodynamic effects (mean ± SD) both with and without a valve.

		Baseline No Valve			Contegra valved conduit		
	MEAN±SD	**EXP**	**PVC25**	**PVC50**	**EXP**	**PVC25**	**PVC50**
P_{TCPC}	***[mm Hg]***	14.1±1.3	14.2±1.8	14.2±1.9	14.2±1.3	14.5±1.8	14.7±2.0
P_{Liver}		15.6±1.6	15.8±2.3	15.8±2.3	15.3±1.7	15.3±2.2	15.1±2.3
Q_{IVC}	**[Lpm]**	2.25±1.6	2.26±2.0	2.29±2.2	2.25±1.5	2.23±1.8	2.26±1.8
Q_{HV}		0.50±1.0	0.51±1.1	0.53±1.2	0.50±0.9	0.50±1.0	0.52±1.0
Q_{svc}		1.14±0.3	1.15±0.5	1.15±0.5	1.15±0.4	1.17±0.5	1.18±0.5
CO		3.39	3.41	3.43	3.40	3.40	3.44
$Q_{ante\ IVC}$		136.2	143.1	148.2	133.4	133.2	136.6
$Q_{retro\ IVC}$		4.34	10.0	13.3	2.0	2.8	4. 5
$\frac{Q_{retro\ IVC}}{Q_{ante\ IVC}}$	***[ml/t$_R$]***	3.2%	7.0%	9.0%	1.5%	2.1%	3.3%
$Q_{ante\ HV}$		36.4	37.3	44.4	35.8	35.4	39.8
$Q_{retro\ HV}$		7.1	9.1	14.2	6.8	6.1	9.7
$\frac{Q_{retro\ HV}}{Q_{ante\ HV}}$		20%	22%	32%	19%	17%	24%
Power Loss	***[mW]***	24.4	26.0	28.2	21.8	22.3	24.7

ASAIO J. Author manuscript; available in PMC 2015 July 01.

Table 3

Hemodynamic effects (mean ± SD) both with and without a valve by increasing pulmonary vascular resistance (PVR).

		Baseline No Valve			Contegra valved conduit		
	MEAN±SD	**EXP**	**PVR33**	**PVR90**	**EXP**	**PVR33**	**PVR90**
P_{TCPC}	***[mm Hg]***	14.1±1.3	15.6±1.3	18.2±1.2	14.2±1.3	15.7±1.2	18.6±1.2
P_{Liver}		15.6±1.6	17.2±1.5	19.7±1.1	15.3±1.7	17.3±1.9	20.0±2.5
Q_{IVC}	**[Lpm]**	2.25±1.6	2.23±1.8	2.16±2.1	2.25±1.5	2.33±1.8	2.38±1.9
Q_{HV}		0.50±1.0	0.48±0.9	0.47±0.9	0.50±0.9	0.47±0.7	0.46±0.8
Q_{svc}		1.14±0.3	1.08±0.4	1.03±0.4	1.15±0.4	1.09±0.5	1.04±0.5
CO		3.39	3.31	3.19	3.40	3.41	3.42
$Q_{ante\ IVC}$		136.2	136.1	134.8	133.4	138.1	141.7
$Q_{retro\ IVC}$		4.34	5.8	8.6	2.0	1.8	2.7
$\frac{Q_{retro\ IVC}}{Q_{ante\ IVC}}$	$[ml/t_R]$	3.2%	4.3%	6.4%	1.5%	1.3%	1.9%
$Q_{ante\ HV}$		36.4	41.3	40.2	35.8	34.8	36.4
$Q_{retro\ HV}$		7.1	13.2	12.7	6.8	7.3	9.5
$\frac{Q_{retro\ HV}}{Q_{ante\ HV}}$		20%	32%	32%	19%	21%	26%